NASA Technical Memorandum 103217

Prediction of the Ullage Gas Thermal Stratification in a NASP Vehicle Propellant Tank Experimental Simulation Using FLOW-3D

Terry L. Hardy and Thomas M. Tomsik
Lewis Research Center
Cleveland, Ohio

July 1990

NASA

Prediction of the Ullage Gas Thermal Stratification in a NASP Vehicle Propellant Tank Experimental Simulation Using FLOW-3D

Terry L. Hardy and Thomas M. Tomsik
NASA Lewis Research Center
Cleveland, Ohio 44135

ABSTRACT

As part of the National Aero-Space Plane (NASP) project, the multi-dimensional effects of gravitational force, initial tank pressure, initial ullage temperature, and heat transfer rate on the two-dimensional temperature profiles were studied. FLOW-3D, a commercial finite-difference fluid flow model, was used for the evaluation. These effects were examined on the basis of previous liquid hydrogen experimental data with gaseous hydrogen pressurant. FLOW-3D results were compared against an existing one-dimensional model. In addition, the effects of mesh size and convergence criteria on the analytical results were investigated. Suggestions for future modifications and uses of FLOW-3D for modeling a NASP tank are also presented.

INTRODUCTION

The temperature distribution in the ullage gas of a tank filled with liquid hydrogen has been of interest for design in both ground and space-based propellant storage systems. The ullage gas temperature distribution is significant in determining the energy distributions and pressurant gas requirements during the ramp pressurization process as well as during the pressurized expulsion of the tank[1-4]. Previous experimental and analytical studies on tank pressurization and expulsion have produced results which show the effects of various parameters on the temperature distributions and pressurant gas quantities required during these processes[5-10]. However, these studies were generally constrained to one-dimensional modeling, and the gravitational forces were limited to those found at ground-level. Current work on the National Aero-Space Plane (NASP) includes the study of fuel tanks which will operate at various gravitational levels with the potential for multi-dimensional thermodynamic effects. As part of the NASP project, slush hydrogen, a mixture of solid and liquid hydrogen, is also being studied[11,12]. Because of the existence of solid particles in the fuel, the use of slush hydrogen may produce thermodynamic effects on both the ullage gas and the propellant not seen using liquid hydrogen propellant. Therefore, a study was initiated

to determine the multi-dimensional effects on the temperature profiles in the ullage gas during the ramp pressurization and expulsion phases on the operation of a NASP vehicle tank.

The FLOW-3D computer code was chosen for modeling the multi-dimensional temperature profiles which occur during tank pressurization. FLOW-3D is a general three-dimensional fluid flow program developed by Flow Science, Inc.[13,14]. The code uses a finite-difference solution of the Navier-Stokes equations based on the Marker-and-Cell (MAC) technique and the Implicit-Continuous Fluid-Eulerian (ICE) technique[15,16]. These techniques were developed through a series of codes with the generic name SOLA. SOLA-VOF, the most successful of these codes, serves as the basis for FLOW-3D; details of SOLA-VOF can be found in reference 17. Capabilities of FLOW-3D include incompressible or fully compressible flow, rotating and accelerating reference frames, and turbulent transport modeling. FLOW-3D has been used extensively to model tank systems, especially systems in which sloshing is involved[18–20].

FLOW-3D CODE SIMULATIONS

The 1988 version of FLOW-3D was used in the present study to determine the temperature profiles during the pressurization phase of operation of a tank. In the pressurization process the tank pressure is gradually increased by the addition of a gas through a diffuser. There is no liquid outflow during pressurization. In a previous experimental study[7] a 5 foot diameter spherical tank filled with liquid hydrogen propellant was pressurized from approximately 17.4 psia to 50 psia using gaseous hydrogen. The tank geometry from this study serves as the basis for the FLOW-3D modeling discussed here. As part of the NASP project, this 5 ft tank geometry will also be used in tests to be performed at K-Site, NASA Lewis Research Center's slush hydrogen test facility located at Plum Brook Station in Sandusky, Ohio[12].

A two-dimensional representation of the 5 foot tank was used in the FLOW-3D simulations with ullage volume percentages of 55%, 28%, and 8.5%, as shown in Figure 1. The simulated ullage was actually a very thin slice taken from the center of the tank; however, because the thickness of the slice was small (0.1 ft), the representation was essentially two-dimensional. The ullage fractions used correspond to actual liquid hydrogen test data discussed in reference 7. In this simulation, hydrogen gas enters the ullage space through a hemispherical diffuser, modeled as a porous obstacle (an option within FLOW-3D). The computational grid used for most cases was a rectangular 10 cell by 10 cell mesh. The wall of the tank cut through this mesh, and the cell size remained constant throughout the mesh for all cases studied.

The velocity of the entering gas used for these simulations was determined from data in reference 7. This velocity was scaled to take the smaller simulated ullage volume into account such that the pressure at the end of the pressurization phase was near 50 psia, corresponding to the previous data. Inlet gas temperatures were also modeled from the previous data: 307°R for the 55% ullage case, 284°R for the 28% ullage, and 524°R for the 8.5% ullage. Pressurization times used in the computations were obtained from previous test data, and for most cases the initial pressure was 17.4 psia. With the exception of the case where the ramp pressurization profiles were examined, the pressurization profile was assumed to be linear. For most cases, the initial ullage gas temperature was assumed to be 250°R at the top of the tank, decreasing linearly to 40°R near the liquid surface. Because instabilities in the code surfaced when a compressible gas was used with the incompressible liquid, only the compressible gas in the ullage was considered (this is known as an "impedance mismatch," occurring when the difference in the densities of the liquid and the gas is great). The liquid surface was assumed to be a rigid plane at a constant temperature. Examples of the input files used are shown in the Appendix for 55%, 28%, and 8.5% ullage cases. Table 1 shows significant input parameters required by FLOW-3D for these simulations, as well as some significant outputs.

For the three ullage volume percents studied, the effects of the following parameters on the ullage temperature profiles at the end of pressurization were examined: gravity level (G), initial tank pressure (P_i), initial ullage temperature (T_i), ramp pressurization profile, and wall (Qwall) and liquid (Qliq) heat transfer rates. In the heat transfer study, the centerline temperatures were also compared against results obtained with SLURP, the NASA Lewis Research Center one-dimensional ramp pressurization code[4]. In addition, results are presented showing effects of convergence criteria (e) and mesh size on FLOW-3D results.

RESULTS

Gravity

Figures 2, 3, and 4 show the effect of variations in the gravitational forces on temperature contours for 55%, 28%, and 8.5% ullage fraction, respectively. The highest and lowest contour temperatures in the mesh are indicated above each graph, and correspond to H and L on the graphs. Ten contours are presented on each graph; the distance between the contours represents a constant difference in temperature, as defined by the high and low temperature. Each figure also includes the convergence criteria and time step ("e" and "dt", respectively) used in the analysis. Each case was run using an initial tank pressure of 17.4 psia and final pressure of 50 psia,

corresponding to the data in the literature. These cases were run assuming no heat transfer to the wall or liquid. The liquid level is indicated by the bottom of the frame. The graph in the upper left-hand corner of Figure 2, at 1-g (G=32.2 ft/sec^2), shows that the final temperature contours (temperatures at the end of pressurization) are quite flat, with a temperature contour range of 376°R near the top of the tank to 109°R near the gas/liquid interface. This indicates a temperature profile which is only axially-dependent, with no radial dependence at 1-g. As the gravitational forces are decreased the temperature profiles begin to show some radial dependence. However, at 55% ullage fraction this dependence does not become significant until the gravitational force is less than 0.1 g (3.22 ft/sec^2). At 0-g the profiles are highly dependent on radius. In addition, the profiles appear to be unsymmetric at 0-g. The unsymmetric profiles may be due to instabilities in the code at low gravitational levels; these instabilities will be discussed later in the report. Note that at 0-g the assumption of a rigid plane at the liquid surface probably does not apply, and a more rigorous analysis would be required in this region.

One possible measure of where gravitational forces become significant is the dimensionless Froude number, Fr, which is defined as

$$Fr = \frac{u^2}{gL}$$

where u is the gas velocity (ft/sec), g is the gravitational force (ft/sec^2), and L is a characteristic length (ft). The Froude number represents a comparison between the inertial forces and the gravitational forces; the inertial forces do not become greater than the gravitational forces until the Froude number is greater than 1. For the tank geometry here, with a flow velocity of approximately 0.5 ft/sec and a characteristic length corresponding to the mesh cell length (approximately 0.25 ft), Fr greater than 1 corresponds to a gravitational force less than 0.1-g. Therefore, the temperature profiles are not expected to show a significant change in shape until the force due to gravity is less than 0.1-g.

Figure 3 (28% ullage) shows a similar result to that obtained with a 55% ullage. At 8.5% ullage, shown in Figure 4, the final temperature profiles become dependent on radius at a higher gravitational level (between 0.1 and 0.5-g). In these runs the high temperature contour is actual greater than the inlet gas temperature. This result was obtained due to adiabatic compression in the tank. In addition, the 8.5% ullage cases appear to exhibit larger differences in high and low temperature contours than those of the 55% or 28% runs, and some unsymmetrical profiles appear at the lower gravitational forces. Code instabilities related to the convergence criteria may be the cause of the unsymmetrical profiles; a discussion of the convergence criteria

will be presented later in the results. Because most applications will probably be at acceleration levels greater than 0.1-g, the FLOW-3D results indicate that the data taken on the ground should apply to the NASP vehicle.

Initial Pressure

In cases where normal boiling point (NBP) liquid hydrogen is the propellant the initial pressure, prior to the ramp pressurization phase, is usually near atmospheric. In the case of slush hydrogen, however, the initial pressure may be as low as 1.1 psia, the triple point pressure of hydrogen. Therefore, because slush hydrogen may be used to fuel the NASP vehicle, the effect of initial pressure on temperature profile was studied. Figure 5 shows a comparison of ullage temperature profiles at the end of pressurization with a 55% ullage at 1-g, with no heat transfer at the wall or liquid. In the top figure, at an initial pressure of 17.4 psia, the final temperature profiles show no radial dependence. At an initial pressure of 1.1 psia, however, the fluid is well mixed (the temperature contours range from 339 to 313°R), and the temperature shows a significant radial dependence at the end of pressurization. The mixing of the ullage gas can be seen in Figure 6, where a comparison is made between the velocity profiles at the two initial pressures (the numbers above the graphs show the scale for velocity vectors, in ft/sec). At an initial pressure of 17.4 psia the velocity of the gas is small near the liquid surface. At 1.1 psia, however, the gas velocity is significant near the gas/liquid interface. Hence, mixing appears to be enhanced at the lower pressures. This enhanced mixing may be the result of a higher pressure drop across the diffuser and hence higher driving force for the flow; however, more work is required to characterize this phenomenon.

Similar results are seen when the ullage fraction is reduced. At 28% ullage and 17.4 psia initial pressure, the temperature is quite stratified, ranging from 373°R to 109°R, as shown in Figure 7. The final profiles at an initial pressure of 1.1 psia show significant mixing and radial dependence, with a temperature contour range of 330 to 306°R. The difference in mixing at the two pressures can be seen in Figure 8, where velocity profiles are compared. The gas appears to penetrate through the ullage to the liquid surface at 1.1 psia, while at 17.4 psia the hydrogen pressurant remains near the diffuser. Finally, Figure 9 shows the temperature comparisons at 8.5% ullage. Here, as in the previous cases, the mixing is enhanced at the lower pressure, leading to less stratification. The temperatures profiles at the low pressure in the 8.5% ullage case do appear to be unsymmetric. The unsymmetric profiles may be due to some computational instabilities not seen at the higher initial pressures. However, the thermal stratification in the ullage appears to be a strong function of the initial tank pressure, regardless of ullage fraction.

Initial Ullage Temperature

Figure 10 shows a comparison of results with two different initial temperature distributions. The cases were run for a 55% ullage at 1-g with no heat transfer considered in the analysis. The top graph shows the final temperature contours when an initial temperature ranging from 250°R near the top of the tank to 40°R at the liquid surface was chosen. The bottom graph shows the results when an initial ullage temperature of 40°R was assumed. From the results it can be seen that, regardless of initial temperature, the profiles produced show no radial dependence. However, the axial distribution of temperature does vary. At an initial temperature of 40°R throughout the tank the final distribution is such that near the top of the tank the temperature is high, but the temperature throughout the rest of the tank is low. In contrast, when a temperature range of 250°R to 40°R is chosen at the start of pressurization, the final distribution is fairly linear, ranging from 376°R at the top to 109°R near the liquid surface. Therefore, it appears that the initial temperature can have a significant effect on the axial temperature profile. This difference will have an effect on the heat transfer at the liquid interface, as the driving force for heat transfer will change with a change in temperature.

Ramp Profiles

Results were also obtained using FLOW-3D to examine the difference in temperature profiles when different pressurization profiles were used. These cases were run using a 55% ullage with no heat transfer to the wall or the liquid. For most cases considered here the pressure was increased at a linear rate, corresponding to a constant inlet gas flow velocity. In an actual pressurization scenario the pressure will probably increase slowly in the initial phase of pressurization, then rapidly increase to reach the final pressure, as discussed in reference 7. Figure 11 shows the two profiles used in the comparison. Ramp Profile 1 is a constant slope profile, with a constant gas velocity. Ramp Profile 2 allows for a slow increase in the flow rate throughout the pressurization time. Figure 12 shows the temperature contours produced using the two profiles. From the figure the shape of the pressure history profile does not have a large impact on the shape of the ullage temperature profile or the magnitude of the resulting temperatures at the end of pressurization. Therefore, for the simple cases shown here, it appears that it is the quantity of gas added, which is approximately the same for both ramp profile cases, and not the rate at which the pressurant is added, which affects the magnitude of the profiles. More effort in this area is required, however, as factors such as initial pressure, mass and heat transfer at the gas/liquid interface, and heat transfer to the wall may impact the results.

Heat Transfer

For the previous cases examined it was assumed that no heat was transferred to the wall or liquid from the gas. In reality, the thermal capacity of the wall as well as the heat transfer to the liquid play key roles in the determination of the stratification of the ullage gas. Therefore, the effect of heat transfer on temperature contours (two-dimensional representations) and centerline temperatures (one-dimensional representation) were investigated.

Heat transfer results are shown in Figure 13 for a tank with 55% ullage. In this figure three cases are considered: no heat transfer (upper left graph), 40 ft-lb/sec (185 BTU/hr) from the gas to the wall and to the liquid (upper right graph), and 80 ft-lb/sec (370 BTU/hr) to the wall and 40 ft-lb/sec to the liquid (bottom graph). The heat transfer rates were chosen based on runs with SLURP, the NASA Lewis Research Center code for calculating tank thermodynamic parameters during slush hydrogen ramp pressurization. The output of SLURP provided heat transfer rates to the wall and the liquid, and these rates were scaled to the FLOW-3D simulation runs based on area.

The results of the heat transfer comparison, as shown in Figure 13, indicate that the heat transfer does not significantly affect the shape of the temperature contours. With heat transfer to the wall and the liquid included, however, the magnitude of the final temperatures of the ullage does decrease by a small amount. The adiabatic solution shows a temperature profile ranging from 376°R near the top of the tank to 109°R near the liquid surface, while the range of temperature contours using 80 ft-lb/sec at the wall is from 370°R to 96°R. In addition, the heat transfer affected the amount of pressurant gas added. Because the final pressure was constant in this study, the amount of mass added had to be increased (velocity was increased) in the cases with heat transfer to meet the 50 psia final pressure criterion.

For comparison of the effects of heat transfer rates at smaller ullage fractions, additional runs were made. Figure 14 shows the results of the comparison for 3 cases: no heat transfer to the wall or liquid (top graph), 40 ft-lb/sec (185 BTU/hr) from the gas to the wall and to the liquid (center graph), and 40 ft-lb/sec to the wall, 60 ft-lb/sec (278 BTU/hr) to the liquid (bottom graph). These cases were run for an 8.5% ullage at 1-g, with an initial pressure of 17.4 psi. The heat transfer rates were chosen based on runs with SLURP, as discussed in the previous figure.

From the output in Figure 14 it can be seen that the heat transfer did not have a significant effect on the shape of the profiles, just as in the case of the 55% ullage. In the case where the heat transfer rate was 60 ft-lb/sec at the liquid surface (bottom

figure) the profiles did show some radial dependence, but the degree of dependence is not high. This radial dependence may be a result of some code instabilities, as will be discussed in the following figures. As expected, as the heat transfer rate was increased the temperature of the ullage gas decreased. Under adiabatic conditions the temperature contours ranged from 627°R to 149°R (top figure). The temperature is higher than the inlet gas temperature due to adiabatic compression. At 60 ft-lb/sec to the liquid the ullage gas temperature ranged from 553°R to 108°R. Therefore, as discussed in the previous section on initial temperature differences, the heat transfer at the interface and axial ullage temperature profiles are related.

Figure 15 shows the comparison of centerline temperatures (the one-dimensional solution) for FLOW-3D runs with and without heat transfer. These results are compared against a similar run with SLURP. For these cases an ullage of 8.5% and an initial pressure of 17.4 psi were used. From the figure it can be seen that the adiabatic solution gave temperatures up to 150°R higher than the solution obtained by SLURP. If, however, a heat transfer to the wall and liquid is chosen such that it is similar to that calculated by SLURP, similar temperature distributions are calculated by FLOW-3D.

It should be noted that the heat transfer rates to wall and to the liquid were input to the FLOW-3D code for study of the tank pressurization problems presented here. In these runs heat transfer to the wall could not be calculated as a mesh large enough to be used to model a volume composed of both a thin wall region and a relatively large ullage space would have been computationally prohibitive. In addition, the "impedance mismatch" between a low density hydrogen gas and a relatively high density liquid hydrogen propellant caused instabilities in the code. This prevented analysis of the heat transfer to the liquid from the gas, and limited the ability to analyze expulsion problems. Therefore, modifications to the basic FLOW-3D code, or a different approach to the problem (such as using FLOW-3D's cylindrical coordinate capability), may be required in order to accurately predict temperature profiles in a NASP vehicle tank without prior experimental knowledge of the mass and heat transfer.

Convergence Criteria

The following figures show the effect of convergence criteria on temperature contour results obtained using FLOW-3D. The simulations were performed using a 55% ullage and an initial pressure of 17.4 psi, with no heat transfer to the wall or the liquid. The comparisons of various convergence criteria were examined both at 1-g and at the analytical asymptote of 0-g. The convergence criterion, e (known as EPSI in the FLOW-3D input), is used to determine the termination of iterations - the iteration

continues until every cell in the computational mesh converges to within this value of e. In the 1988 version of FLOW-3D the time step, dt (DELT in the input), and the convergence criterion are related because of stability limits on the code. Therefore, as the convergence criterion is decreased the time step must also be decreased.

Figure 16 shows the effect of convergence criteria at 1-g. From the figure it can be seen that for the various convergence criteria used, .02, .002, and 1 x 10^{-6}, there is little difference in the results. The ullage temperature contours range from 376°R at the top of the tank to 110-120°R near the gas/liquid interface. Although the temperature profile near the midpoint of the ullage differs somewhat between the cases considered, the convergence criteria does not seem to significantly affect the temperature distribution results at 1-g. This result is confirmed by a comparison of the centerline temperatures, as shown in Figure 17. Note however that in some cases, such as those shown for the 8.5% ullage fraction, a loose convergence criteria (large value of "e") may lead to code instabilities for the geometry chosen.

Figure 18 shows the effect of convergence criteria at 0-g. In this figure the results at a convergence criteria of 1x10^{-6} is quite different from the results at e=0.02. From the figure it appears that the temperature contours are more symmetrical at e=1x10^{-6} compared to the result with e=0.02. The symmetrical temperature distribution is a result of an "even" distribution of the gas. The difference in velocity profiles, as shown in Figure 19, indicates that the gas is evenly distributed when a convergence criterion of 1x10^{-6} is chosen (lower graph). At larger values of "e" this symmetrical distribution of the gas is not evident. A symmetrical temperature distribution is probably a realistic result for the geometry considered here; therefore, it is recommended that a tight convergence criterion be used at low gravitational levels (a much more computationally costly requirement) and that a loose convergence criterion be used for most cases at 1-g.

Mesh Size

The following figures show the effect of mesh size on temperature contours. The results shown were for 55% ullage at 1-g and zero-g with an initial pressure of 17.4 psi, pressure convergence criterion (e) of .02 psi, and a time step (dt) of .005 sec. There was no heat transfer to the wall or liquid in these cases. Two mesh sizes were considered: a 100 cell mesh (10x10) and a 400 cell mesh (20x20). From the results shown in Figure 20 the mesh size did not impact the shape or the magnitude of the final temperature profiles to any large degree, although there was some difference near the liquid surface. From results presented in the Figure 21, however, mesh size appears to have a significant effect on temperature distribution at zero-g. In this case the 10x10 mesh may not be large enough to resolve the gas velocity profiles in

the tank. Therefore, if a low gravitational force is used a finer partitioning of the tank volume should be used (at the cost of high CPU time). At ground conditions, however, a smaller number of mesh cells appears adequate.

FUTURE FLOW-3D MODIFICATIONS

In order to use the FLOW-3D code for a complete analysis of the NASP vehicle tank several modifications to the code should be implemented. The ability to model the heat and mass transfer at the gas/liquid interface appears to be a critical capability in determining the gas requirements, the slush hydrogen solid losses, and the degree of thermal stratification in the ullage[3]. The addition of this capability may require modification of the code to include the ability to perform calculations during expulsion, when the fluid dynamics of the liquid and the thermodynamics of the gas are both important. In addition, because the NASP vehicle may use both helium and hydrogen gas during the pressurization and expulsion phases, a two-component ullage model should be added. Finally, an initial slush hydrogen fluid dynamics model has been added to the FLOW-3D code[14]. However, this model will require improvements to fully model slush hydrogen dynamics, including an improved slush melting/solidification capability, the ability to have a free surface (gas/liquid interface) present when the slush model is used, and the capability of modeling slush hydrogen with a gaseous pressurant (3 phases simultaneously).

CONCLUDING REMARKS

The FLOW-3D computer code was used to determine the effects of various parameters on the two-dimensional temperature profiles during ramp pressurization prior to pressurized expulsion of a liquid hydrogen tank. These results apply to the NASP vehicle tanks where multi-dimensional effects may be important. The results obtained can be summarized as follows:

1. For 1-g and for an initial pressure near atmospheric, the ullage gas final temperatures do not show a radial dependence. As the gravitational forces are reduced, the profiles do not show a significant radial dependence until the gravitational forces are less than 0.1-g.

2. Initial tank pressure has a significant impact on the temperature distribution. At an initial pressure of 17.4 psi the final ullage temperature profile was not dependent

on radius. At an initial pressure of 1.1 psi the final temperatures indicated that the fluid was well-mixed, and the profiles appeared to be radially dependent.

3. The initial temperature affects only the magnitude of the final temperatures in the ullage.

4. The shape of the ramp pressurization profile did not significantly impact the final temperature profiles.

5. Convergence criteria and mesh size seem to make the largest difference in results at low gravitational levels. Tighter convergence criteria and smaller mesh sizes are recommended at low gravitational levels to prevent the potential for computational instabilities.

6. Centerline temperatures using the SLURP one-dimensional pressurization code and the FLOW-3D program matched when heat transfer rates obtained by SLURP were scaled and used as input to the FLOW-3D simulations.

As the current effort was intended to be an initial investigation of FLOW-3D, further analysis is required to determine the optimal approach in using the code to analyze tank pressurization and expulsion problems. In addition, future efforts should include the use of some of the unique capabilties of FLOW-3D, such as the simulation of tank sloshing or the evaluation of the dynamics of the liquid hydrogen. Although modifications are required to the code to simulate slush hydrogen tank thermodynamics, FLOW-3D has been shown to be a versatile tool which may be used for future studies of the NASP storage and feed system.

REFERENCES

1. Roudebush, W.H., "An Analysis of the Problem of Tank Pressurization During Outflow", NASA TN D-2585, 1965.

2. Ring, E., "Pressurizing Gas Thermodynamics" in Rocket Propellant and Pressurization Systems, Chapter 18, Prentice-Hall, Inc., Englewood Cliffs, N. J., 1964.

3. Tomsik, T.M., Hardy, T.L., and Moran, M., "EXPL: A Computer Code for Prediction of Tank Conditions During Slush Hydrogen Pressurized Expulsion Using Gaseous Hydrogen Discharge," NASP Contractor Report 1060, August, 1989.

4. Hardy, T.L., and Tomsik, T.M., "SLURP: A Computer Code for Pressurization of a Slush Hydrogen Tank Using Gaseous Hydrogen or Helium," NASP Technical Memorandum 1088, January, 1990.

5. Epstein, M. "Prediction of Liquid Hydrogen and Oxygen Pressurant Requirements," Adv. Cryogenic Engineering, Vol. 10, Plenum Press, N.Y.,1964.

6. Masters, P. A., "Computer Programs for Pressurization (RAMP) and Pressurized Expulsion from a Cryogenic Liquid Propellant Tank," NASA TN D-7504, July, 1974.

7. Stochl, R.J., et al., "Gaseous-Hydrogen Requirements for the Discharge of Liquid Hydrogen from a 1.52-meter (5-ft)- Diameter Spherical Tank," NASA TN D-5336, August, 1969.

8. Stochl, R.J., et al., "Gaseous-Helium Requirements for the Discharge of Liquid Hydrogen from a 1.52-meter (5-ft)- Diameter Spherical Tank," NASA TN D-5621, January, 1970.

9. Stochl, R.J., et al., "Gaseous-Hydrogen Requirements for the Discharge of Liquid Hydrogen from a 3.96-meter (13-ft)- Diameter Spherical Tank," NASA TN D-5387, August, 1969.

10. Cady, E.C., Flaska, T.L., and Worrell, P.K., "In-Tank Thermodynamics of Slush Hydrogen for the National Aerospace Plane," Advances in Cryogenic Engineering, Vol. 35, Plenum Press, NY, 1989, p. 1755.

11. Hannum, N.P., "Technology Issues Associated With Fueling The National Aerospace Plane With Slush Hydrogen", presented at the 7th Joint Intersociety Cryogenic Conference Symposium, cosponsored by ASME, AIChE, and IIR, Houston, TX, Jan. 22-26, 1989, NASA TM 101386.

12. DeWitt, R.L., et al., "Slush Hydrogen (SLH2) Technology Development for Application to the National Aerospace Plane (NASP)," Cryogenic Engineering Conference, Los Angeles, CA, July-24-28, 1989, NASA TM 102315.

13. Navickas, J., "Prediction of a Liquid Tank Thermal Stratification by a Finite Difference Computing Method," AIAA/ASEE/ASME/SAE 24th Joint Propulsion Conference, Boston, MA, July 11-14, 1988.

14. Navickas, J., Cady, E.C., and Flaska, T.L., "Modeling of Solid-Liquid Circulation in the National Aerospace Plane's Slush Hydrogen Tanks," AIAA/ASEE/ASME/SAE 24th Joint Propulsion Conference, Boston, MA, July 11-14, 1988.

15. Harlow, F.H., and Welch, J.E., "Numerical Calculation of Time-Dependent Viscous Incompressible Flow," Phys. Fluids, Vol. 8, 1965, p. 2182.

16. Harlow, F.H., and Amsden, A.A., "A Numerical Fluid Dynamics Calculation Method for All Flow Speeds," J. Computational Physics, Vol 8., 1971, p. 197.

17. Hirt, C.W., and Nichols, B.D., "Volume of Fluid (VOF) Method for the Dynamics of Free Boundaries," J. Computational Physics, Vol. 39, 1981, p. 201.

18. Watkins, W.B., and Hussey, R.G., "Spin-Up from Rest in a Cylinder," Phys. Fluids, Vol. 20, 1977, pp. 1596-1604.

19. Eastes, T.W., et al., "Zero-Gravity Slosh Analysis," Proc. ASME Winter Annual Meeting, Miami, FL, November, 1985.

20. Sicilian, J.M, and Hirt, C.W., "Numerical Simulation of Propellant Sloshing for Spacecraft," Proc. ASME Winter Annual Meeting, New Orleans, LA, Dec. 9-14, 1984.

APPENDIX: Sample Input Files For FLOW-3D Runs

Example Input File for a 55% Ullage Case

```
  K-SITE LH2: 55% Ullage, G=32.2,Pi=17.4,Ti=250,
$XPUT
 ITB=0, EPSI=0.02, IPDIS=0, DELT=0.005, DTMAX=0.05,
 SPRTDT=4.0, PRTDT=5.0, PLTDT=4.0,
 WB=2, WT=6, WF=1, WBK=1, WL=1, WR=1,
 TWFIN=24.0, GZ=-32.2,
 IPUN=10, IHTC=1, IFENRG=2,
 AUTOT=0.0,
    TIMBCT(1)=0.0,   TIMBCT(2)=0.2,   TIMBCT(3)=100.0,
    TBCT(1,6)=307.0, TBCT(2,6)=307.0, TBCT(3,6)=307.0,
    TBCT(1,5)=40.0,  TBCT(2,5)=40.0,  TBCT(3,5)=40.0,
    TBCD=307.,
    WBCT(1,6)=0.0,   WBCT(2,6)=-0.60, WBCT(3,6)=-0.60,
    PBCT(1,6)=3600., PBCT(2,6)=3600., PBCT(3,6)=3600.0,
    FBCT(1,6)=0.0,   FBCT(2,6)=0.0,   FBCT(3,6)=0.0,
    POBCT(1,5)=-40., POBCT(2,5)=-40., POBCT(3,5)=-40.,
    ICMPRS=1,        IADIX=1,         IADIZ=1,
    RF2=24690.96,    CV2=53335.0,
$END
$MESH
 PX(1)=-2.5,   PX(2)=0.0,   PX(3)=2.5,
 SIZEX(2)=0.25,
 NXCELL(1)=5,  NXCELL(2)=5, NXCELT=10,
 PY(1)=0.0,    PY(2)=0.10,  NYCELT=1,
 PZ(1)=-0.187, PZ(2)=2.5,   NZCELT=10,
$END
$OBS
 NOBS=2,
 CC(1)=6.25,    CX2(1)=-1.0, CZ2(1)=-1.0,
 IOH(1)=1,      RAL(1)=0.5,
 CC(2)=6.0,     CX2(2)=1.0,    CZ2(2)=1.0,  CZ(2)=-5.0,
 OPOR(2)=0.7,   IOH(2)=1,
 TOBS(1)=0.0,   TOBS(2)=100.0,
 POBS(1,1)=-40.,POBS(2,1)=-40.,
$END
$FL
  PRESI=2500.0,
$END
$BF
$END
$TEMP
  NTMP=1, ITDIS(1)=1,
  TCC(1)=-52.82, TCZ=121.1, TZH(1)=2.5, TZL(1)=0.75,
$END
$MOTN
$END
$GRAFIC
 NVPLTS=1,  JV1(1)=2,    JV2(1)=2,
 NCPLTS=1,  KONTYP(1)=5, JC1(1)=2,   JC2(1)=2,
$END
$PARTS
$END
```

Example Input File for a 28% Ullage Case

```
  K-SITE LH2: 28% Ullage, G=32.2,Pi=17.4,Ti=250,
$XPUT
 ITB=0, EPSI=0.007, IPDIS=0, DELT=0.005, DTMAX=0.5,
 SPRTDT=4.0, PRTDT=5.0, PLTDT=4.0,
 WB=2, WT=6, WF=1, WBK=1, WL=1, WR=1,
 TWFIN=24.0, GZ=-32.2,
 IPUN=10, IHTC=1, IFENRG=2,
 AUTOT=0.0,
    TIMBCT(1)=0.0,   TIMBCT(2)=0.2,   TIMBCT(3)=100.0,
    TBCT(1,6)=284.0, TBCT(2,6)=284.0, TBCT(3,6)=284.0,
    TBCT(1,5)=40.0,  TBCT(2,5)=40.0,  TBCT(3,5)=40.0,
    TBCD=307.,
    WBCT(1,6)=0.0,   WBCT(2,6)=-0.323,WBCT(3,6)=-0.323,
    PBCT(1,6)=3600., PBCT(2,6)=3600., PBCT(3,6)=3600.0,
    FBCT(1,6)=0.0,   FBCT(2,6)=0.0,   FBCT(3,6)=0.0,
    ICMPRS=1,        IADIX=1,         IADIZ=1,
    RF2=24690.96,    CV2=51732.0,
$END
$MESH
 PX(1)=-2.5,   PX(2)=0.0,   PX(3)=2.5,
 SIZEX(2)=0.25,
 NXCELL(1)=5,  NXCELL(2)=5, NXCELT=10,
 PY(1)=0.0,    PY(2)=0.10,  NYCELT=1,
 PZ(1)=0.75,   PZ(2)=2.5,   NZCELT=10,
$END
$OBS
 NOBS=2,
 CC(1)=6.25,  CX2(1)=-1.0, CZ2(1)=-1.0,
 IOH(1)=1,
 RAL(1)=0.5,
 CC(2)=6.0,   CX2(2)=1.0,  CZ2(2)=1.0,  CZ(2)=-5.0,
 OPOR(2)=0.7, IOH(2)=1,
 TOBS(1)=0.0, TOBS(2)=100.0,
$END
$FL
  PRESI=2500.0,
$END
$BF
$END
$TEMP
  NTMP=1, ITDIS(1)=1,
  TCC(1)=-52.82, TCZ=121.1, TZH(1)=2.5, TZL(1)=0.75,
$END
$MOTN
$END
$GRAFIC
 NVPLTS=1,  JV1(1)=2,   JV2(1)=2,
 NCPLTS=1,  KONTYP(1)=5,
 JC1(1)=2,   JC2(1)=2,
$END
$PARTS
$END
```

Example Input File for an 8.5% Ullage Case

```
  K-SITE LH2: 8.5% Ullage, G=0.0,Pi=17.4,Ti=250,
$XPUT
 ITB=0, EPSI=0.05, IPDIS=0, DELT=0.003, DTMAX=0.05,
 SPRTDT=4.0, PRTDT=5.0, PLTDT=4.0,
 WB=2, WT=6, WF=1, WBK=1, WL=1, WR=1,
 TWFIN=15.0, GZ=0.0,
 IPUN=10, IHTC=1, IFENRG=2,
 AUTOT=0.0,
    TIMBCT(1)=0.0,   TIMBCT(2)=0.2,   TIMBCT(3)=100.0,
    TBCT(1,6)=524.0, TBCT(2,6)=524.0, TBCT(3,6)=524.0,
    TBCT(1,5)=40.0,  TBCT(2,5)=40.0,  TBCT(3,5)=40.0,
    TBCD=307.,
    WBCT(1,6)=0.0,   WBCT(2,6)=-0.197,WBCT(3,6)=-0.197,
    PBCT(1,6)=3600., PBCT(2,6)=3600., PBCT(3,6)=3600.0,
    FBCT(1,6)=0.0,   FBCT(2,6)=0.0,   FBCT(3,6)=0.0,
    ICMPRS=1,        IADIX=1,         IADIZ=1,
    RF2=24690.96,    CV2=63833.0,
$END
$MESH
 PX(1)=-1.8,   PX(2)=0.0,   PX(3)=1.8,
 SIZEX(2)=0.25,
 NXCELL(1)=5,  NXCELL(2)=5, NXCELT=10,
 PY(1)=0.0,    PY(2)=0.10,  NYCELT=1,
 PZ(1)=1.60,   PZ(2)=2.5,   NZCELT=10,
$END
$OBS
 NOBS=2,
 CC(1)=6.25,  CX2(1)=-1.0, CZ2(1)=-1.0,
 IOH(1)=1,
 RAL(1)=0.5,
 CC(2)=6.0,   CX2(2)=1.0,  CZ2(2)=1.0,  CZ(2)=-5.0,
 OPOR(2)=0.7, IOH(2)=1,
 TOBS(1)=0.0, TOBS(2)=100.0,
$END
$FL
  PRESI=2500.0,
$END
$BF
$END
$TEMP
  NTMP=1, ITDIS(1)=1,
  TCC(1)=-338.0, TCZ=235.0, TZH(1)=2.5, TZL(1)=1.60,
$END
$MOTN
$END
$GRAFIC
 NVPLTS=1,  JV1(1)=2,   JV2(1)=2,
 NCPLTS=1,  KONTYP(1)=5,
 JC1(1)=2,   JC2(1)=2,
$END
$PARTS
$END
```

Table 1: Major Input and Output Parameters for FLOW-3D Tank Pressurization Runs

Inputs	Outputs
Time Step	Cell Temperature
Convergence Criteria	Cell Pressure
Gravitational Level	Cell Gas Velocity
Initial Ullage Temperature	Average Ullage Pressure
Initial Pressure	Fluid Density
Heat Transfer to Liquid	Dynamic Viscosity
Heat Transfer to Wall	
Inlet Gas Velocity	
Inlet Gas Temperature	
Gas Specific Heat	
Mesh Definition	
Obstacle Definition	

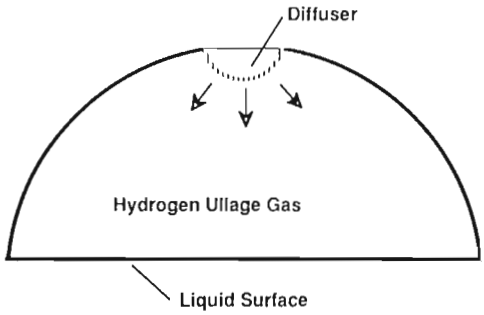

FIGURE 1. - FLOW-3D MODEL OF K-SITE TANK PRESSURIZATION.

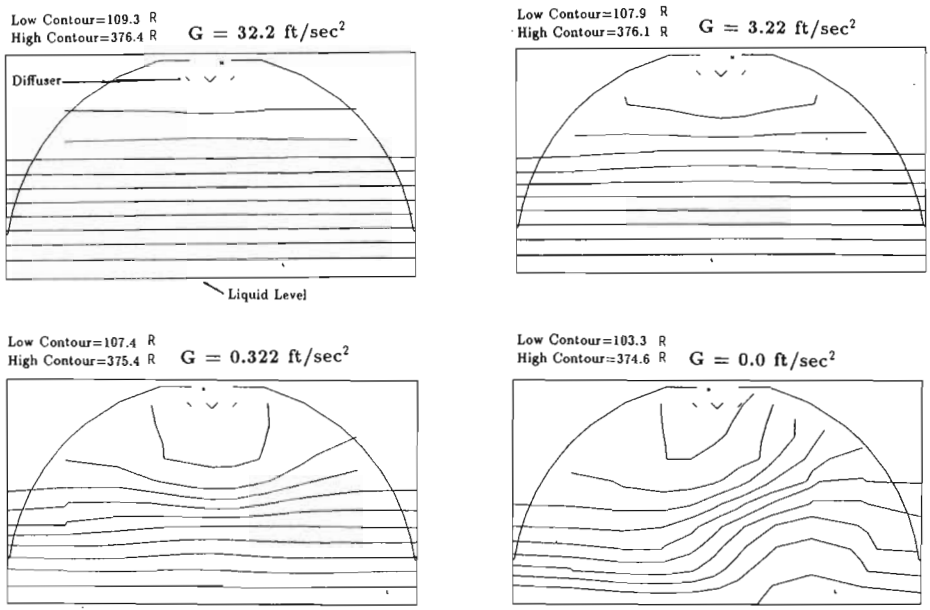

FIGURE 2. - EFFECT OF GRAVITY ON TEMPERATURE CONTOURS, 55 PERCENT ULLAGE, P_i = 17.4 PSI, e = .02, dt = 0.005 SEC, 24 SEC PRESSURIZATION.

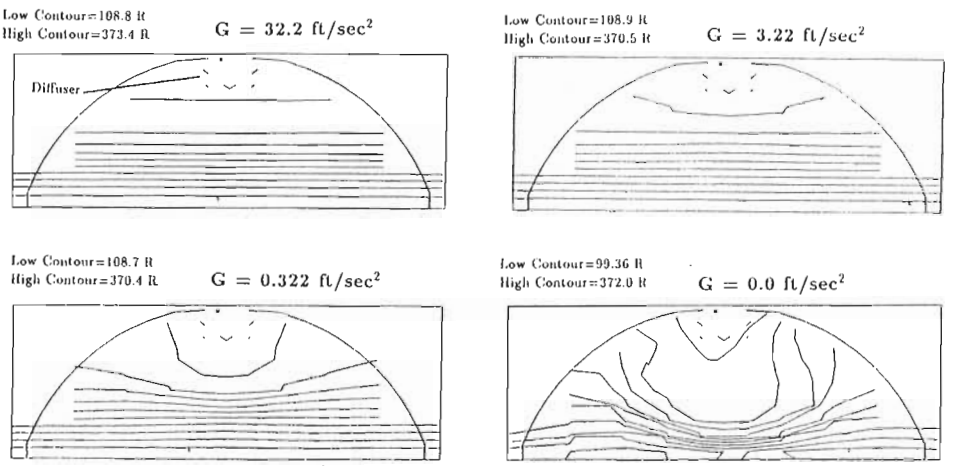

FIGURE 3. - EFFECT OF GRAVITY ON TEMPERATURE CONTOURS, 28 PERCENT ULLAGE, P_i = 17.4 PSI, e = .007, dt = .005 SEC, 24 SEC PRESSURIZATION.

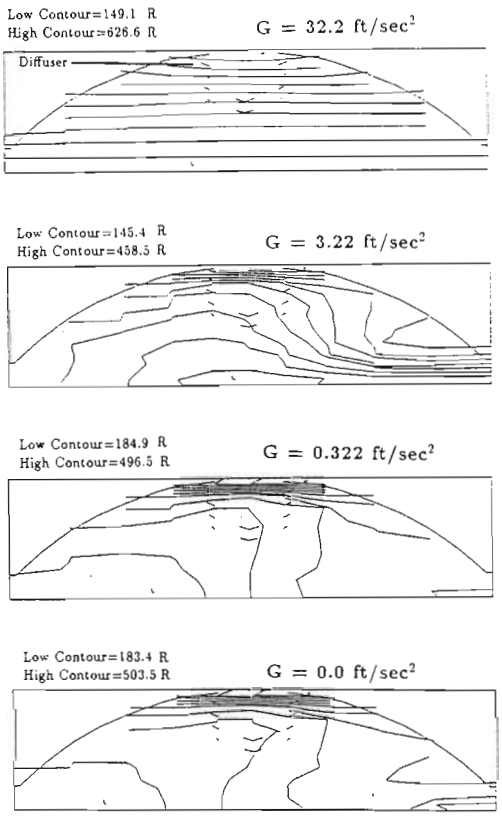

FIGURE 4. - EFFECT OF GRAVITY ON TEMPERATURE CONTOURS, 8.5 PERCENT ULLAGE, P_i = 17.4 PSI, e = .05, dt = .003 SEC, 15 SEC PRESSURIZATION.

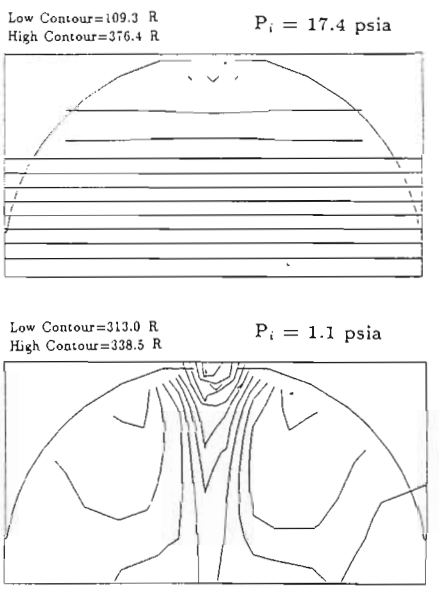

FIGURE 5. - EFFECT OF INITIAL PRESSURE ON TEMPERATURE CONTOURS, 55 PERCENT ULLAGE, G = 32.2 FT/SEC^2, e = .02, dt = .005 SEC, 24 SEC PRESSURIZATION.

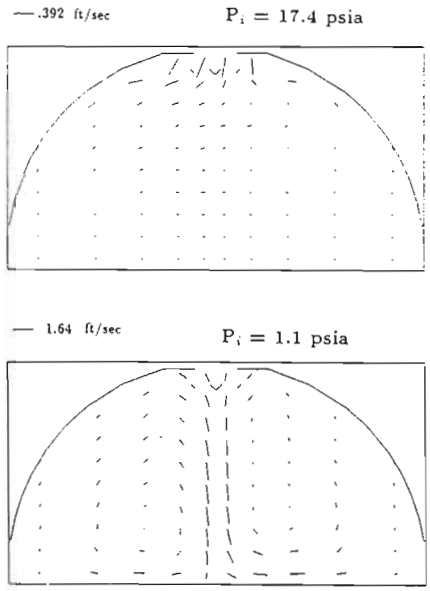

FIGURE 6. - EFFECT OF INITIAL PRESSURE ON VELOCITY PROFILE, 55 PERCENT ULLAGE, G = 32.2 FT/SEC^2, e = .02, dt = .005 SEC, 24 SEC PRESSURIZATION.

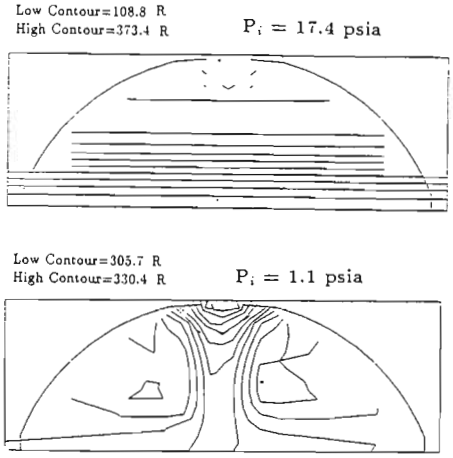

FIGURE 7. - EFFECT OF INITIAL PRESSURE ON TEMPERATURE CONTOURS, 28 PERCENT ULLAGE, G = 32.2 FT/SEC^2, e = .007, dt = .005 SEC, 24 SEC PRESSURIZATION.

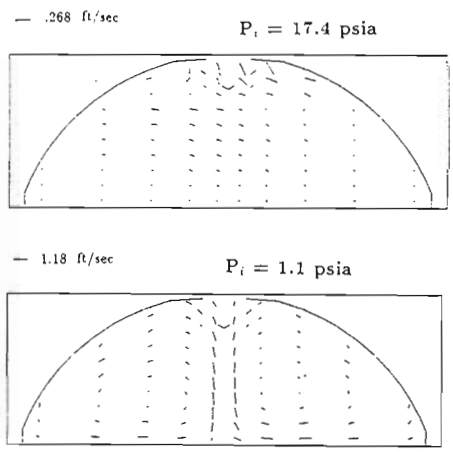

FIGURE 8. - EFFECT OF INITIAL PRESSURE ON VELOCITY PROFILE, 28 PERCENT ULLAGE, P_i = 17.4 PSI, e = .007, dt = .005 SEC, 24 SEC PRESSURIZATION.

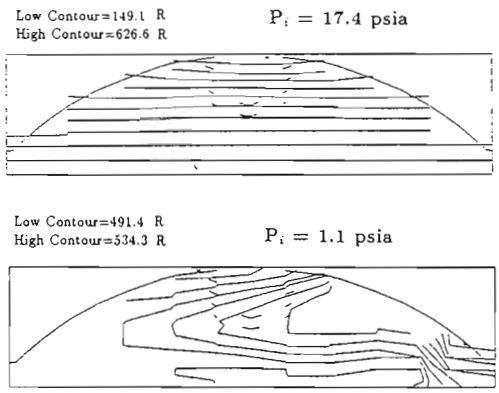

FIGURE 9. - EFFECT OF INITIAL PRESSURE ON TEMPERATURE CONTOURS, 8.5 PERCENT ULLAGE, G = 32.2 FT/SEC^2, e = .05, dt = .003 SEC, 15 SEC PRESSURIZATION.

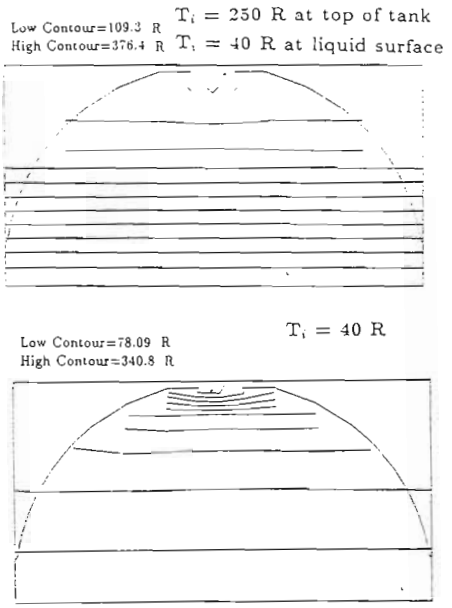

FIGURE 10. - EFFECT OF INITIAL TEMPERATURE ON TEMPERATURE CONTOURS, 55 PERCENT ULLAGE, P_i = 17.4 PSI, G = 32.2 FT/SEC^2, e = .02, 24 SEC PRESSURIZATION.

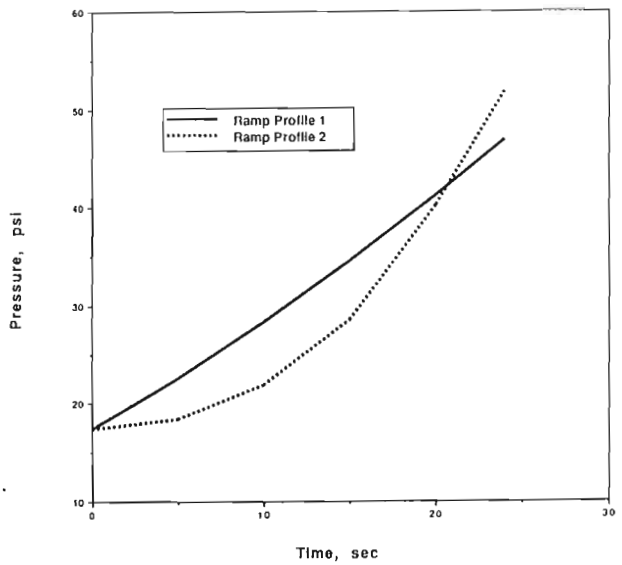

FIGURE 11. - RAMP PROFILES USED FOR TEMPERATURE PROFILE COMPARISON, 55 PERCENT ULLAGE, P_i = 17.4 PSI, 24 SEC PRESSURIZATION.

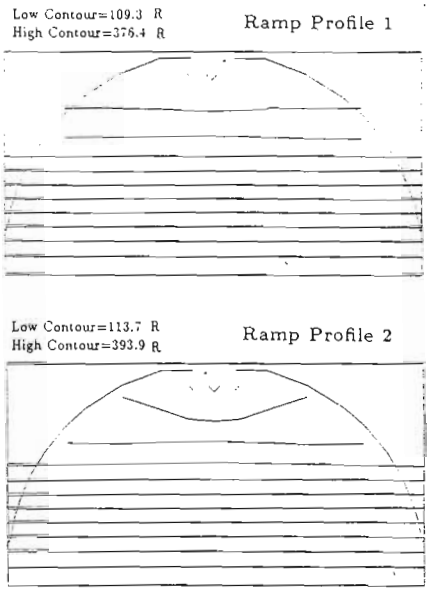

FIGURE 12. - EFFECT OF RAMP RATE ON TEMPERATURE CONTOURS, 55 PERCENT ULLAGE, P_i = 17.4 PSI, G = 32.2 FT/SEC^2, e = .02, dt = .005 SEC, 24 SEC PRESSURIZATION.

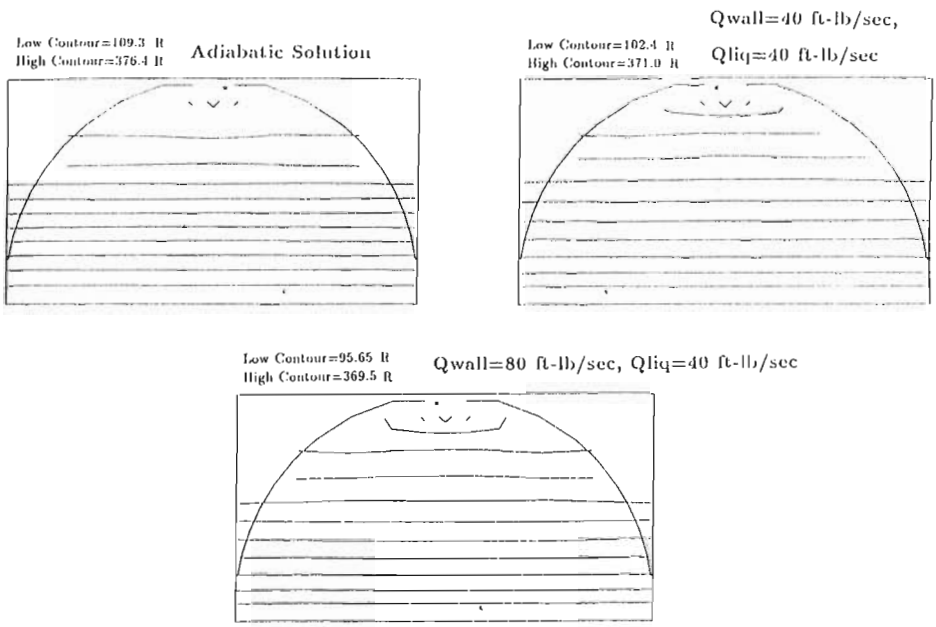

FIGURE 13. - EFFECT OF HEAT TRANSFER ON TEMPERATURE CONTOURS, 55 PERCENT ULLAGE, P_i = 17.4 PSI, G = 32.2 FT/SEC^2, e = .02, dt = .005 SEC, 24 SEC PRESSURIZATION.

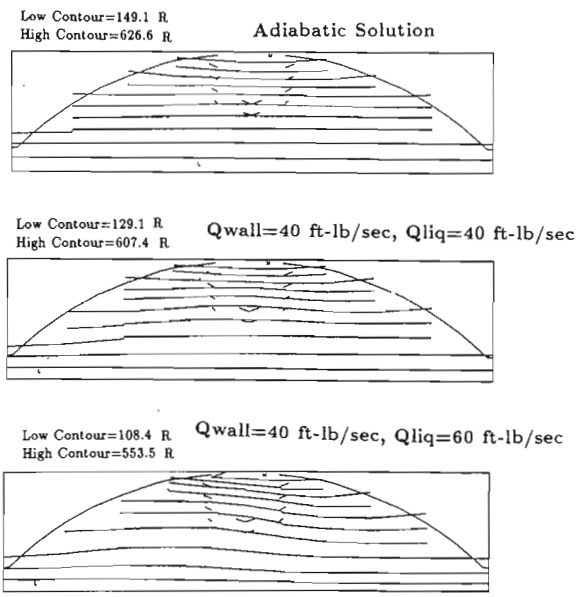

FIGURE 14. - EFFECT OF HEAT TRANSFER ON TEMPERATURE CONTOURS, 8.5 PERCENT ULLAGE, P_i = 17.4 PSI, G = 32.2 FT/SEC^2, e = .05, dt = .003 SEC, 15 SEC PRESSURIZATION.

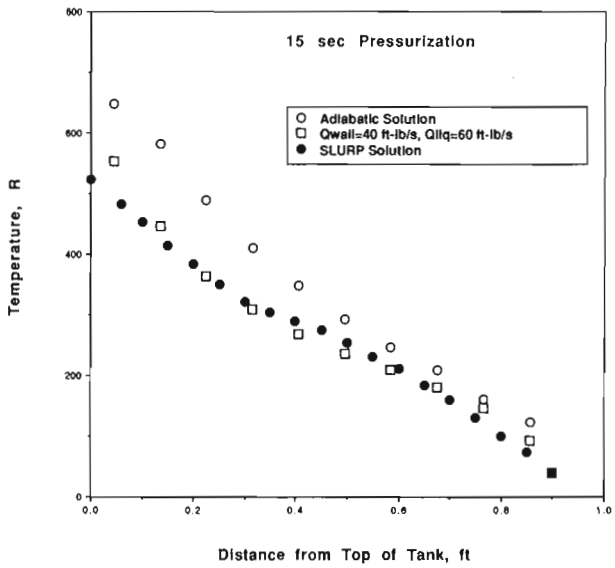

FIGURE 15. - COMPARISON OF CENTERLINE TEMPERATURES USING VARIOUS HEAT TRANSFER RATES, 8.5 PERCENT ULLAGE, e = .07, dt = .005 SEC, P_i = 17.4 PSI.

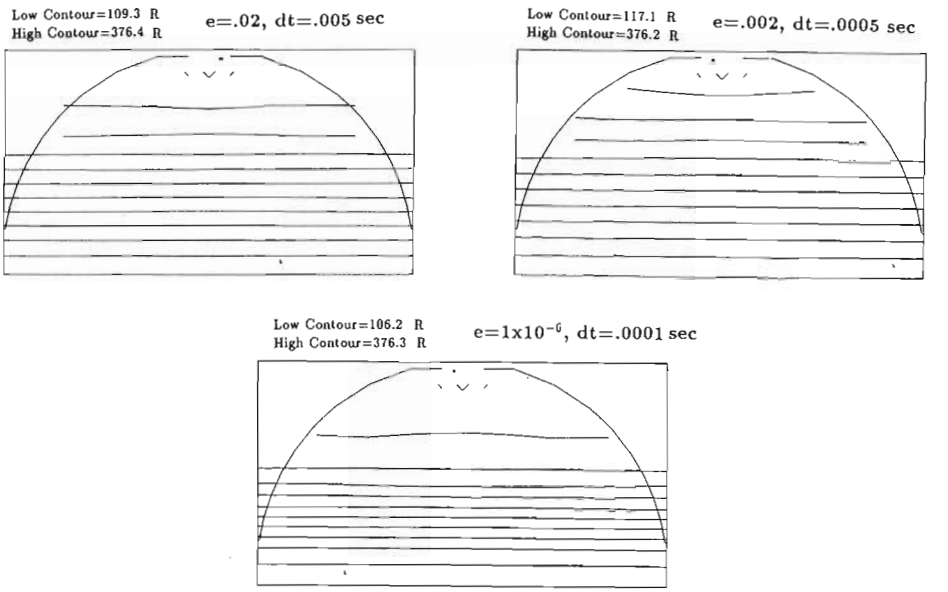

FIGURE 16. - EFFECT OF CONVERGENCE CRITERIA ON TEMPERATURE CONTOURS, 55 PERCENT ULLAGE, P_i = 17.4 PSI, G = 32.2 FT/SEC^2, 24 SEC PRESSURIZATION.

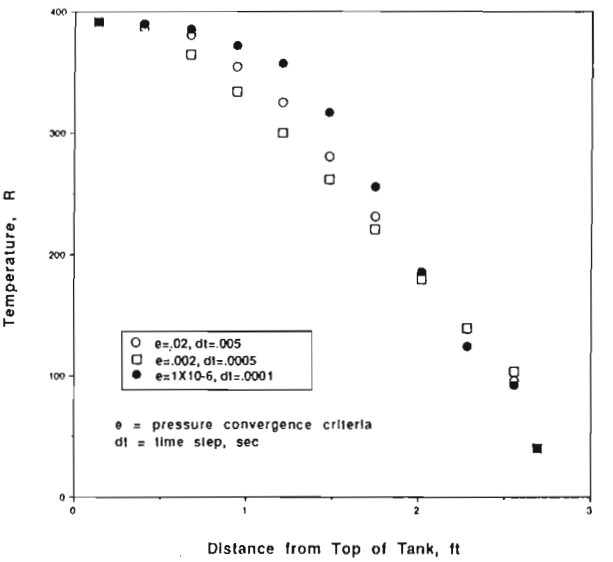

FIGURE 17. - COMPARISON OF CENTERLINE TEMPERATURES USING VARIOUS CONVERGENCE CRITERIA, 55 PERCENT ULLAGE, G = 32.2 FT/SEC^2, P_i = 17.4 PSI, 24 SEC PRESSURIZATION.

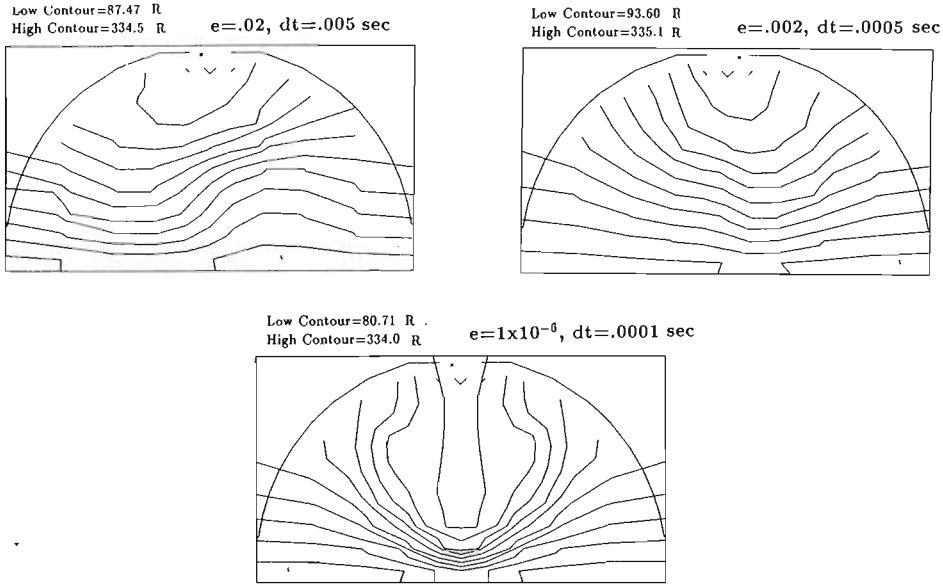

FIGURE 18. - EFFECT OF CONVERGENCE CRITERIA ON TEMPERATURE CONTOURS, 55 PERCENT ULLAGE, P_i = 17.4 PSI, G = 0.0 FT/SEC^2, 16 SEC PRESSURIZATION.

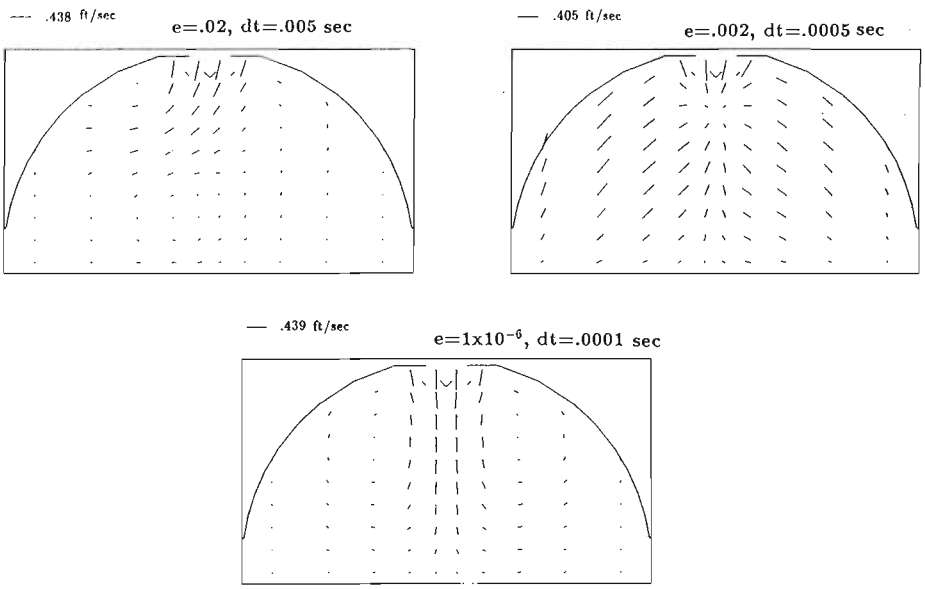

FIGURE 19. - EFFECT OF CONVERGENCE CRITERIA ON VELOCITY PROFILE, 55 PERCENT ULLAGE, P_i = 17.4 PSI, G = 0.0 FT/SEC^{2}M 16 SEC PRESSURIZATION.

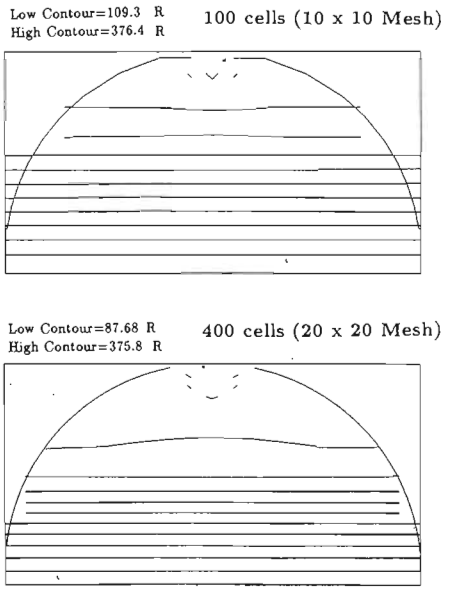

FIGURE 20. - EFFECT OF MESH SIZE ON TEMPERATURE CONTOURS, 55 PERCENT ULLAGE, P_i = 17.4 SEC, G = 32.2 FT/SEC^2, e = .02, dt = .005 SEC, 24 SEC PRESSURIZATION.

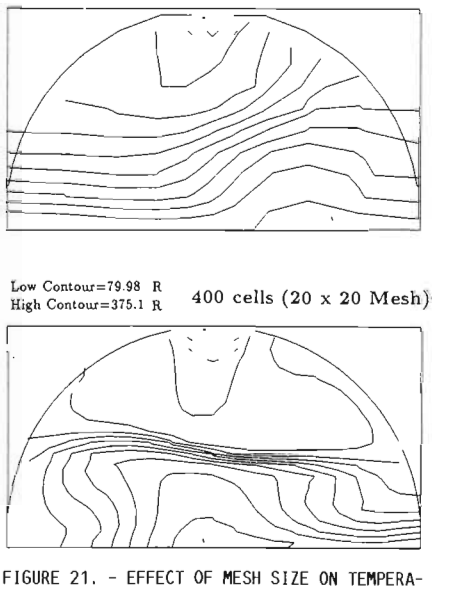

FIGURE 21. - EFFECT OF MESH SIZE ON TEMPERATURE CONTOURS, 55 PERCENT ULLAGE, P_i = 17.4 PSI, G = 0.0 FT/SEC^2, e = .02, dt = .005 SEC, 24 SEC PRESSURIZATION.

NASA
National Aeronautics and Space Administration

Report Documentation Page

1. Report No.	2. Government Accession No.	3. Recipient's Catalog No.
NASA TM-103217		

4. Title and Subtitle	5. Report Date
Prediction of the Ullage Gas Thermal Stratification in a NASP Vehicle Propellant Tank Experimental Simulation Using FLOW-3D	July 1990
	6. Performing Organization Code

7. Author(s)	8. Performing Organization Report No.
Terry L. Hardy and Thomas M. Tomsik	E-5629
	10. Work Unit No. 763-01-21

9. Performing Organization Name and Address	11. Contract or Grant No.
National Aeronautics and Space Administration Lewis Research Center Cleveland, Ohio 44135-3191	
	13. Type of Report and Period Covered Technical Memorandum

12. Sponsoring Agency Name and Address	14. Sponsoring Agency Code
National Aeronautics and Space Administration Washington, D.C. 20546-0001	

15. Supplementary Notes

16. Abstract

As part of the National Aero-Space Plane (NASP) project, the multi-dimensional effects of gravitational force, initial tank pressure, initial ullage temperature, and heat transfer rate on the two-dimensional temperature profiles were studied. FLOW-3D, a commercial finite-difference fluid flow model, was used for the evaluation. These effects were examined on the basis of previous liquid hydrogen experimental data with gaseous hydrogen pressurant. FLOW-3D results were compared against an existing one-dimensional model. In addition, the effects of mesh size and convergence criteria on the analytical results were investigated. Suggestions for future modifications and uses of FLOW-3D for modeling of a NASP tank are also presented.

17. Key Words (Suggested by Author(s))	18. Distribution Statement
NASP; Slush hydrogen; Hydrogen; Propellant tanks; Thermal stratification; Computational fluid dynamics; Computer programming; Numerical analysis	Unclassified – Unlimited Subject Category 28

19. Security Classif. (of this report)	20. Security Classif. (of this page)	21. No. of pages	22. Price*
Unclassified	Unclassified	26	A03

*For sale by the National Technical Information Service, Springfield, Virginia 22161